Talanta 217 (2020) 121043

Contents lists available at ScienceDirect

Talanta

journal homepage: www.elsevier.com/locate/talanta

Rapid LA-REIMS and comprehensive UHPLC-HRMS for metabolic phenotyping of feces

Lieven Van Meulebroek[a], Simon Cameron[b,c], Vera Plekhova[a], Margot De Spiegeleer[a], Kathleen Wijnant[a,d], Nathalie Michels[d], Stefaan De Henauw[d], Bruno Lapauw[e], Zoltan Takats[b], Lynn Vanhaecke[a,c,*]

[a] Ghent University, Faculty of Veterinary Medicine, Department of Veterinary Public Health and Food Safety, Laboratory of Chemical Analysis, Salisburylaan 133, 9820, Merelbeke, Belgium
[b] Imperial College London, Faculty of Medicine, Department of Metabolism, Digestion, and Reproduction, Division of Systems Medicine, St. Dunstans Road, London, SW7 2AZ, United Kingdom
[c] Queen's University Belfast, School of Biological Sciences, Lisburn Road 97, Belfast, United Kingdom
[d] Ghent University, Faculty of Medicine and Health Sciences, Department of Public Health and Primary Care, Corneel Heymanslaan 10, 9000, Gent, Belgium
[e] Ghent University Hospital, Department of Endocrinology, Corneel Heymanslaan 10, 9000, Ghent, Belgium

ARTICLE INFO

Keywords:
Laser-assisted rapid evaporative ionization mass spectrometry
Ultra-high performance liquid chromatography high-resolution mass spectrometry
Fecal metabolomics
Type 2 diabetes mellitus

ABSTRACT

Ambient ionization-based techniques hold great potential for rapid point-of-care applicable metabolic fingerprinting of tissue and fluids. Hereby, feces represents a unique biospecimen as it integrates the complex interactions between the diet, gut microbiome and host, and is therefore ideally suited to study the involvement of the diet-gut microbiome axis in metabolic diseases and their treatments at a molecular level. We present a new method for rapid (< 10 s) metabolic fingerprinting of feces, *i.e.* laser-assisted rapid evaporative ionization mass spectrometry (LA-REIMS) with an Nd:YAG laser (2940 nm) and quadrupole Time-of-Flight mass spectrometer as main components. The LA-REIMS method was implemented on mimicked crude feces samples from individuals that were assigned a state of type 2 diabetes or euglycaemia. Based on the generated fingerprints, enclosing 4923 feature ions, significant segregation according to disease classification was achieved through orthogonal partial least squares discriminant analysis ($Q^2(Y)$ of 0.734 and *p*-value of $1.93e^{-17}$) and endorsed by a general classification accuracy of 90.5%. A comparison between the discriminative performance of the novel LA-REIMS and our established ultra-high performance liquid-chromatography high-resolution MS (UHPLC-HRMS) metabolomics and lipidomics methodologies for fingerprinting of stool was performed. Based on the supervised modelling results upon UHPLC-HRMS ($Q^2(Y) \geq 0.655$ and *p*-value $\leq 4.11\ e^{-5}$), equivalent or better discriminative performance of LA-REIMS fingerprinting was concluded. Eventually, comprehensive UHPLC-HRMS was employed to assess metabolic alterations as observed for the defined classes, whereby metformin treatment of the type 2 diabetes patients was considered a relevant study factor to acquire new mechanistic insights. More specifically, ten metabolization products of metformin were identified, with (hydroxylated) triazepinone and metformin-cholesterol reported for the first time *in vivo*.In conclusion, LA-REIMS was established as an expedient strategy for rapid metabolic fingerprinting of feces, whereby potential implementations may relate, but are not limited to differential diagnosis and treatment efficacy evaluation of metabolic diseases. Yet, LC-HRMS remains essential for in-depth biological interpretation.

* Corresponding author. Ghent University, Faculty of Veterinary Medicine, Department of Veterinary Public Health and Food Safety, Laboratory of Chemical Analysis, Salisburylaan 133, 9820, Merelbeke, Belgium.
E-mail addresses: Lieven.VanMeulenbroek@ugent.be (L. Van Meulebroek), S.Cameron@imperial.ac.uk, S.Cameron@qub.ac.uk (S. Cameron), Vera.Plekhova@ugent.be (V. Plekhova), Margot.DeSpiegeleer@ugent.be (M. De Spiegeleer), Kathleen.Wijnant@ugent.be (K. Wijnant), Nathalie.Michels@ugent.be (N. Michels), Stefaan.DeHenauw@ugent.be (S. De Henauw), Bruno.Lapauw@uzgent.be (B. Lapauw), z.takats@imperial.ac.uk (Z. Takats), Lynn.Vanhaecke@Ugent.be, L.Vanhaecke@qub.ac.uk (L. Vanhaecke).

https://doi.org/10.1016/j.talanta.2020.121043
Received 4 December 2019; Received in revised form 1 April 2020; Accepted 13 April 2020
Available online 14 April 2020
0039-9140/

1. Introduction

The concept of ambient ionization mass spectrometry (AIMS) is generally referred to as any ionization technique that is performed under open-air conditions and in conjunction with any kind of mass spectrometry. Hereby, samples can be analyzed in their native environment or after minimal pre-treatment, substantiating the simplicity of the analytical workflow [1]. This is in strong contrast with the more conventional analytical approaches of liquid-chromatography mass spectrometry (LC-MS), which are typically associated with an extensive workflow of sample homogenization, aliquoting, extraction, purification, and pre-concentration [2,3]. As a result, translation of these hyphenated MS-techniques into point-of-care testing is very unlikely because the conditions are very different to those of laboratory testing [4]. As such, AIMS may be assigned significant value to advance the actual transition from laboratory testing into point-of-care testing in non-laboratory settings. This would empower clinicians to make fast decisions and address challenges on health disparities in order to improve healthcare delivery [4,5]. In this context, a wide range of applications have been actualized, *i.e.* surgical interventions where real-time diagnostic AIMS analysis is performed to support per-operative decisions while intersecting malignant tumors [1,6–9]. For this kind of *in vivo* applications, relatively few techniques have been demonstrated qualified, including laser-assisted rapid evaporative ionization MS (LA-REIMS) [10,11]. The process of laser ablation itself is based on the laser-emitted infrared wavelength regime that excites the most intense vibrational band (oxygen-hydrogen stretching mode) of water molecules that are contained by the tissue under investigation, initiating matrix-assisted desorption and ionization of intact biomolecules [11]. Following this principle, we presumed that LA-REIMS also holds potential for rapid analysis of biofluids such as blood, urine, and feces, all comprising a high percentage of water. LA-REIMS fingerprinting of biofluids would offer unique opportunities for healthcare practice as insights on the pathophysiological status may be acquired during consultation, while the patient is still on-site. As such, in any decentralized setting, LA-REIMS may significantly aid in diagnosis of disease and selection of treatment, tailored towards an individual's metabolic fingerprint and associated phenotype [12]. However, it should be mentioned that metabolite characterization by LA-REIMS is typically based on accurate mass measurements only (i.e. MS^1), which has significant implications for metabolite identification and to some extent also absolute quantitation. Although MS^2 scan events may be appended to increase selectivity and identification power, the lack of chromatographic separation will complicate interpretation of these MS^2 spectra, as isobaric and isomeric compounds will contribute to an aggregated MS^2 spectrum. In addition, the lack of chromatographic separation may typically be accompanied by severe ion suppression effects, which may also hamper accurate quantification [13]. As a consequence, biofluid metabolomics by LA-REIMS may primarily find acceptance in first-line differentiation of samples based on distinctive fingerprints and according to (patho)physiological state. For a more detailed read-out of the metabolome, conventional LC-MS approaches are more eligible as advanced separation and in-depth characterization of metabolites may be achieved. This allows for absolute quantitation and high-confidence identification, which enables biological interpretation and pathway analysis. As such, rapid LA-REIMS in complement with comprehensive LC-MS may strongly advance the positioning of metabolomics as a present-day practice in the clinic. As an alternative, the hyphenation of REIMS with ion mobility also holds promise to increase selectivity [13].

In this study, our first objective was to establish and exploit LA-REIMS for rapid screening of human fecal samples to uncover relevant metabolic alterations in relation to our disease classification (glycemic index HbA1c). Hereby, feces was selected as biospecimen as its inherent metabolome captures the complex interactions between the host, diet and gut microbiome, and thus encloses unique potential for fingerprinting, as had already been demonstrated by conventional UHPLC-HRMS for multiple (gastrointestinal) diseases [14–17]. To assess the inherent fingerprinting capacities of LA-REIMS, we performed cross-platform evaluations with UHPLC-HRMS, assessing the similarity in terms of metabolome coverage and metabotyping discriminative power. A second objective was to exploit the available UHPLC-HRMS data in relation to the cohort characteristics to acquire new mechanistic insights, with as major objective to support the hypothesis that UHPLC-HRMS remains indispensable for pathway analysis and in-depth biological interpretations.

2. Materials and methods

2.1. Biological material

Fecal samples were acquired from men and women, which were assigned a state of euglycaemia (36 individuals, average age of 47 ± 9 years, BMI of 23.6 ± 3.5, 65.2% women) or type 2 diabetes (38 individuals, average age of 61 ± 8 years, BMI of 30.2 ± 3.8, 25.0% women). Classification was in essence based on a threshold criterion of 60 mmol/mol glycated hemoglobin A1c (HbA1c), being measured using venous whole blood and HPLC [18]. Participants were recruited at Ghent University and Ghent University Hospital, whereby the main exclusion criteria were the presence of chronic disorders (with exception of the typical co-morbidities of type 2 diabetes), acarbose or glucagon-like-peptide 1 therapy, and recent antibiotics treatment. Stool samples were lyophilized for 48 h and subsequently homogenized and sieved to attain representative aliquots, which were stored at −80 °C until analysis. The study was approved by the UZ Ghent Ethical Committee (EC 2016/0673), with samples being collected during two sampling campaigns (September–October 2016; April–May 2017). It may be noted that the established classes exhibited some discrepancies with respect to age, BMI, and gender, whereby their confounding impact was estimated to be quite limited, although no definite exclusion of confounding behaviors could be concluded (Supplemental Table 1). In this regard, the terminology of 'disease classification' was used throughout this paper to refer to the classification that was based on the glycemic index HbA1c but for which some covariates may occur. With respect to the latter, this also included the treatment of metformin, which type 2 diabetes patients received.

2.2. Metabolic fingerprinting by LA-REIMS

Analytical method. For LA-REIMS analysis, 200 ± 0.5 mg lyophilized fecal material was transferred into a 2 mL microcentrifuge tube and thoroughly mixed with 600 μL ultrapure water to mimic the composition of a fresh sample. This mixture was spread on a microscope slide and subjected to laser ablation. The system used was an Opolette™ HE2940 pump laser (OPOTEK, LLC), connected to a laser power supply (OPOTEK, LLC) and consisting of an Nd:YAG laser, steering optics, optical parametric oscillator (fixed at 2940 nm), and wavelength separation optics. Transmission of the laser energy to the sample was achieved through free space optics, enfolding a line of metallic-coated mirrors (OptoSigma Global Top) and Plano-convex lens (Thorlabs). Main operational settings of the laser pumping system concerned a pulse time of 180 μs and repetition rate of 20 Hz. The aerosol produced was transferred to the REIMS-platform by a polytetrafluorethylene tubing (3.2 mm O.D., 1.6 mm I.D.), which was connected to the REIMS interface by means of a T-shaped piece. This T-piece was directly hyphenated to the transfer capillary and allowed the inflow of isopropanol, containing the internal standards palmitic acid-d_{31} (5 ng/μL, $[M - H]^-$) and 1,2-dimyristoyl-d_{54}-sn-glycero-3-phosphocholine (100 ng/μL, $[M+H]^+$). The flow rate was set at 0.15 mL/min for negative and 0.125 mL/min for positive ionization, and achieved using a 11 Elite syringe pump (Harvard Apparatus). Mass analysis was carried out by a Xevo G2-XS Quadrupole Time-of-Flight (QToF) mass spectrometer (Waters Corporation), with the cone voltage

(40 V), heater bias voltage (40 V for positive and 70 V for negative ionization), scan time (0.3 s), and *m/z* scan range (from 50 to 1200 Da) being the main parameters. The total acquisition time was 0.5 min per sample, whereby at least two burns (± 3 s per burn) were generated.

Measures for quality assurance. The REIMS instrument was calibrated in sensitivity mode according to the manufacturer's standard instructions (Waters Corporation), using a 0.5 mM sodium formate solution of isopropanol and water (90/10, v/v) at a flow rate of 0.1 mL/min. Calibration enabled high mass accuracy measurements with mass deviations < 3 ppm. Prior to analysis of the actual samples, a pool of feces (n = 10) was run ten times in both polarity modes for conditioning of the LA-REIMS instrument. Experimental samples were run in a random order as a single batch, whereby instrument performance was monitored based on the internal standards.

Data analysis. LA-REIMS data were processed using the MassLynx® V4.1 Progenesis® Bridge tool (Waters Corporation), thereby performing lock mass correction, background subtraction, creation of extracted ion chromatograms for each burn, and separation of multiple burns. Definition of the individual burns was generally based on a total ion current (TIC) replicate threshold of 10,000,000 arbitrary units (au), whereby the data from the most intense burn were retained for subsequent processing by Progenesis® QI V2.3 (Waters Corporation), using the automatic sensitivity method for peak picking (sensitivity value of 3). The associated data matrices were TIC-normalized and subjected to multivariate statistical analysis using SIMCA 14.1 (Umetrics), for which data were log-transformed and pareto-scaled. The applied scaling approach was selected as a compromise between mean centering and autoscaling, for which the range of feature intensities could be standardized to some extent without inflating baseline noise [19,20]. This was considered important to maximize the robustness of the marker signature, accountable for differentiation of disease classification. Principal component analysis (PCA-X) was applied to evaluate natural clustering of samples and reveal potential outliers based on the 95% Hotelling's T^2 criterion. Orthogonal partial least squares discriminant analysis (OPLS-DA) was used to differentiate samples according to pathophysiological state in a supervised fashion. Validity of the OPLS-DA models was assessed by permutation testing, cross-validated analysis of variance (*p*-value < 0.05), and the quality parameter $Q^2(Y)$ (≥0.5) [21].

2.3. Metabolic fingerprinting by UHPLC-HRMS

Analytical method 1. Lipidomic fingerprints were acquired by implementing the protocol of Van Meulebroek et al. (2017) [17], which allows holistic coverage of the non-polar fraction of the fecal metabolome. A maximum of about 60 samples per working day and person could be extracted, with an instrumental acquisition time of 20 min per sample, measuring metabolites with an *m/z*-value between 67 and 1200 Da. In brief, 200 ± 0.5 mg of lyophilized feces was subjected to liquid-liquid extraction based on methanol and methyl *tert*-butyl ether, both containing butylated hydroxytoluene. Phase separation was induced by adding ultrapure water, containing trichloroacetic acid, whereby the upper layer was collected and evaporated to dryness. The residue was re-suspended in a solution of chloroform and methanol. A 5-μL aliquot was subjected to chromatographic separation using a Dionex Ultimate 3000 XRS UHPLC system (Thermo Fisher Scientific) that was equipped with an Acquity BEH phenyl column (Waters Corporation, 2.1 × 150 mm, 1.7 μm). Hereby, a binary solvent system consisting of ultrapure water and methanol, both acidified with ammonium acetate, was used to establish a 20-min gradient elution program. A constant flow rate of 300 μL/min and column oven temperature of 40 °C were set. MS analysis was carried out on a high-resolution hybrid quadrupole Q-Exactive™ orbitrap mass spectrometer (Thermo Fisher Scientific), preceded by heated electrospray ionization (HESI-II) that operated in polarity switching mode. Instrumental settings for full-scan analysis were a sheath gas flow rate of 40 au, auxiliary gas flow rate of 10 au, sweep gas flow rate of 2 au, heater and capillary temperature of both 325 °C, S-lens RF level of 80%, and spray voltage of 3.5 kV for positive and 3.0 kV for negative ionization mode. The mass resolution was 70,000 full width at half maximum (FWHM; 1 Hz), automatic gain control (AGC) 2×10^5 ions, and maximum injection time 50 ms.

Analytical method 2. Polar metabolomics analyses were performed according to the methodology of De Paepe et al. (2018) [22], developed to cover a variety of chemical classes with polar functional groups. Also here, 60 samples could be extracted per day and person. The acquisition time was 18 min, measuring metabolites with an *m/z*-value between 53.4 and 800 Da. In brief, 200 ± 0.5 mg of lyophilized feces was subjected to solid-liquid extraction, using ultrapure water and methanol as extraction solvents. The supernatant was purified by means of a polyamide filter (0.45 μm pore size) and diluted by ultrapure water. A 10-μL aliquot was injected in the above-mentioned LC-system, that was equipped with a Acquity HSS T3 column (Waters Corporation, 2.1 × 150 mm, 1.8 μm). Hereby, a binary solvent system consisting of ultrapure water and acetonitrile, both acidified with formic acid, was applied to establish an 18-min gradient profile. A constant flow rate of 0.4 mL/min and column oven temperature of 45 °C were set. MS analysis was performed on a Q-Exactive™ orbitrap mass spectrometer (Thermo Fisher Scientific), preceded by electrospray ionization (HESI-II) in polarity switching mode. Instrumental settings were a sheath gas flow rate of 50 au, auxiliary gas flow rate of 25 au, sweep gas flow rate of 3 au, a heater temperature of 350 °C, a capillary temperature of 250 °C, an S-lens RF level of 50%, and a spray voltage of 4 kV for both ionization modes. The mass resolution was 140,000 FWHM, the AGC 1 x e^6, and the maximum injection time 70 ms.

Measures for quality assurance. Instrument calibration was performed by infusing ready-to-use calibration mixtures (Thermo Fisher Scientific), warranting accurate mass measurement with deviations below 3 ppm. Additionally, to check the operational conditions in terms of sensitivity and chromatographic performance, customized standard mixtures of > 100 target analytes were injected for method 1 and 2 [17,22]. Moreover, to adjust for instrumental fluctuations that may occur throughout the sequence run, quality control (QC) samples were incorporated [23]. QC samples were constructed by pooling equal extract aliquots from all samples. These samples were run at the beginning of the analytical run to stabilize the system and at regular intervals within the batch of biological samples, and included two variants of QC-samples in accordance with the defined subpopulations.

Data analysis. For compiling the metabolic fingerprints, full-scan data were processed by Sieve™ 2.2 software (Thermo Fisher Scientific), performing alignment and peak picking. As primary parameters, a maximum retention time shift of 0.5 min, a minimum intensity threshold of 1,000,000 au, and an *m/z* step size of 6 ppm were set. The acquired peak intensity data were first TIC-normalized to adjust for sample-specific analytical bias and afterwards normalized using the QC-samples to adjust for feature-specific analytical bias. With respect to the latter, the intensity of each feature was divided by the average intensity of that feature, as calculated from the next two QC-samples. Multivariate statistical analysis was performed using SIMCA 14.1 (Umetrics), for which data were pareto-scaled and log-transformed.

2.4. Identification of potential UHPLC-HRMS metabolite markers

Identification of marker molecules was based on the accurate *m/z*-value of the molecular ion, isotope profile (^{13}C and ^{34}S), and fragmentation spectrum. With respect to the latter, parallel reaction monitoring MS/MS experiments (PRM, using an inclusion list) were conducted whereby following settings were applied; *m/z* isolation width of 0.5 Da, mass resolution of 17,500 full width at half maximum, automatic gain control target of $2e^5$, and collision energies between 10 and 80 eV. Analysis of fragmentation data was based on SIRIUS 4.0, MetFrag, mzCloud, and in-house fragmentation libraries. Reported identities reached Tier 1 or 2 [24].

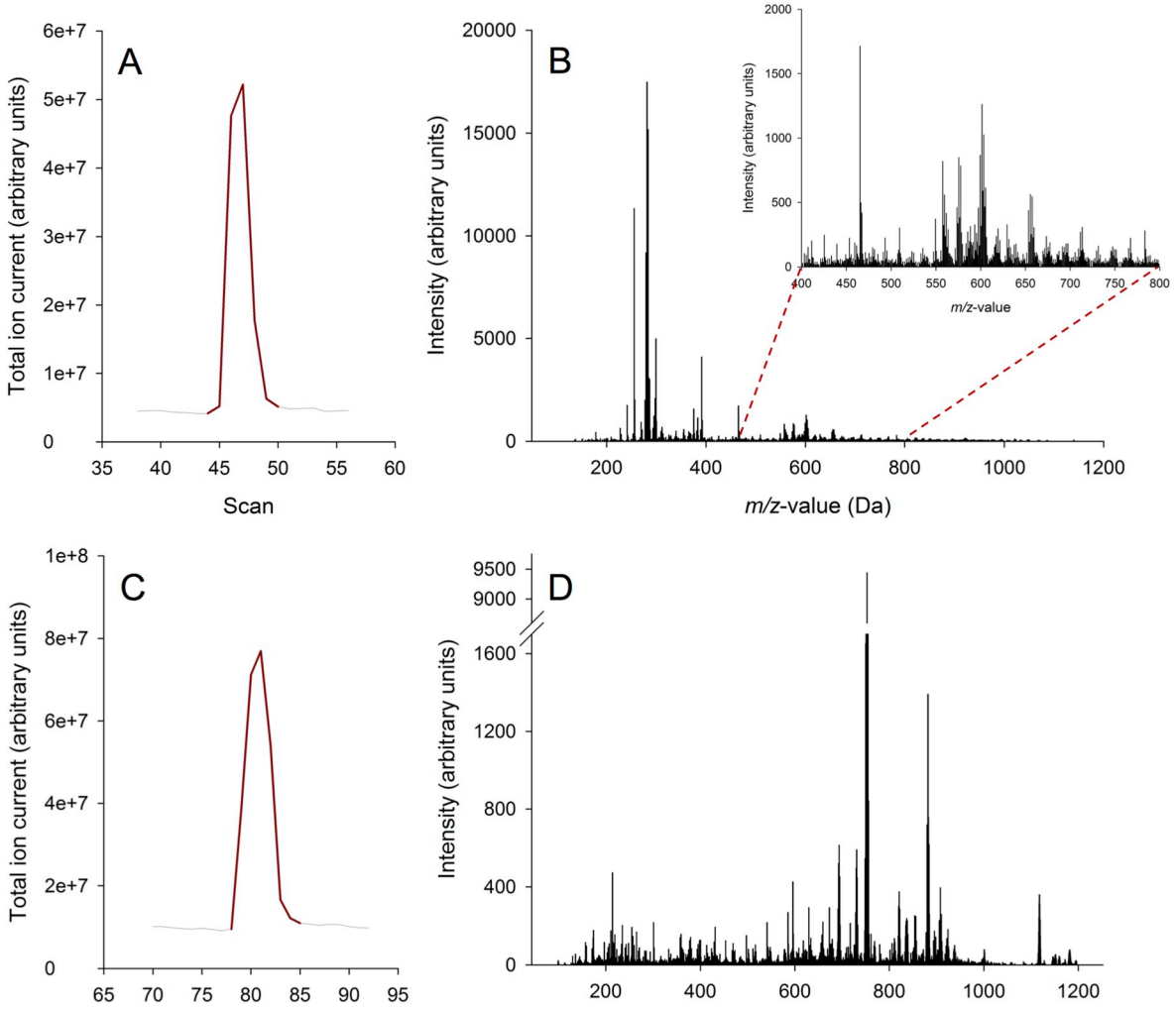

Fig. 1. LA-REIMS analysis of feces. Total ion current as recorded by the REIMS platform upon laser ablation of a fecal sample for negative (A) and positive (C) ionization. The period of irradiation is indicated in red whereas the grey line represents the background during periods that no ablation was carried out. Overall MS spectrum as acquired during ablation for negative (B) and positive (D) ionization. (For interpretation of the references to colour in this figure legend, the reader is referred to the Web version of this article.)

3. Results

3.1. Metabolic fingerprinting by LA-REIMS

Metabolome coverage. Using LA-REIMS, a total of 4923 unique features were detected within the selected scan range, including 2166 negative and 2757 positive ions. Grouping of the features into components (i.e. clusters of related features) was not performed because the lack of LC-separation would lead to a high number of false positives. As such, the total number of features may be seen as a reflection of the maximum coverage possible. The metabolic fingerprints, as obtained for each ionization mode, are presented in Fig. 1.

Discriminative performance. Multivariate analysis was performed combining the data from both ionization modes. OPLS-DA modelling revealed significant clustering according to disease classification (valid permutation testing, a *p*-value of 1.93 e^{-17}, and a $Q^2(Y)$ of 0.734), which was strengthened by unsupervised PCA-X analysis (Fig. 2). The ability of LA-REIMS to accomplish discriminative fingerprinting was further substantiated by a general classification accuracy of 90.5% and class type 2 diabetes sensitivity of 89.5% and specificity of 91.7%, as being verified by a five-fold 20%-leave-out validation strategy. Subsequently, the biomarker signature was assessed whereby 52 feature ions were assigned marker potential (VIP $>$ 1, correlation $|pcorr| > 0.5$, covariance $|p| > 0.03$, and Jack-knifed confidence intervals not across zero) [25,26]. It was noted that the majority of these features (53.7%) were situated within the 450–650 Da mass window, typically being populated by phosphoglycerolipids, sphingolipids, fatty acids, and glycerolipids. In addition, based on the accurate mass and in line with the findings of the UHPLC-HRMS approach, one marker was tentatively identified as metformin (PubChem CID4091) (the first-line drug in the treatment of type 2 diabetes). Nevertheless, a valid OPLS-DA model ($Q^2(Y)$ of 0.0.524 and *p*-value of 4.04 e^{-9}) could also be constructed after exclusion of metformin and related compounds (*i.e.* those compounds with a VIP-score $\geq$ 2 when performing OPLS-modelling with the Y-variable being the metformin abundance). It should be noted, however, that metabolic changes induced by metformin treatment may still exert their influence.

Throughout analysis, TIC-normalized signal intensities as measured for the internal standards palmitic acid-d_{31} and 1,2-dimyristoyl-d_{54}-sn-glycero-3-phosphocholine showed a coefficient of variance of 28.4% and 39.2%, respectively. Incorporation of QC-samples at regular intervals across the batch of biological samples could offer additional means to correct for instrumental instability.

3.2. Metabolic fingerprinting by UHPLC-HRMS

Metabolome coverage. Metabolic fingerprints were constructed based on the full-scan data as obtained from the second sampling campaign,

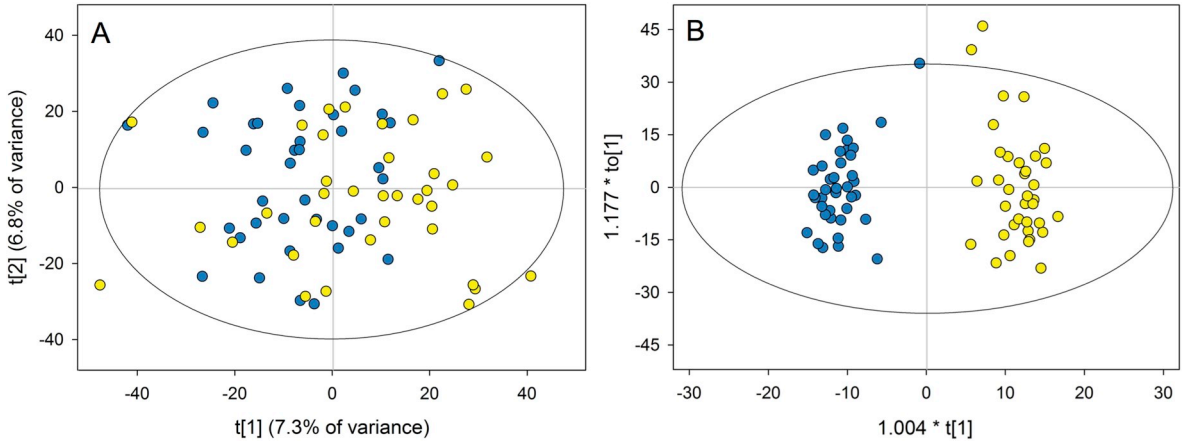

Fig. 2. Discriminative performance of LA-REIMS fecal fingerprinting in type 2 diabetes. PCA-X score plot that was generated based on the LA-REIMS data from the type 2 diabetes study participants (blue) and controls (yellow) (A). Score plot that was generated based on the validated OPLS-DA model (Q^2 of 0.734), consisting of one predictive and two orthogonal principal components (B). (For interpretation of the references to colour in this figure legend, the reader is referred to the Web version of this article.)

including 42 participants of which half were diagnosed with type 2 diabetes. It should be noted that the dataset from the first sampling campaign was not used as being acquired with another LC pumping system, which turned out to significantly affect chromatographic outcomes. Shifts in retention time could not be remediated as this would require adjustments of the alignment settings (*i.e.* an increased maximum allowed retention time shift), which would be accompanied by the substantial misalignment of closely eluting but unique chromatographic peaks. Using the polar metabolomics strategy, a total of 7630 unique feature ions was detected, whereby the majority (*i.e.* 72.03%) was acquired in positive ionization mode. Taking into consideration the presence of ^{13}C isotopes as well as the occurrence of multiple adducts, 3580 unique components were determined. Using the lipidomics approach, a total of 26,512 lipophilic feature ions was detected, of which the majority was observed in positive ionization mode (*i.e.* 75.86%). Evaluation of the isotopes and adducts yielded 17,119 unique components. Calculation of the total metabolome coverage was not possible due to the overlap in polarity range between the polar metabolomics (logP from −4.8 to 9.7) and lipidomics (logP from −2.7 to 16.2) methodology, implying that a large number of metabolites was covered by both methods.

Discriminative performance. Multivariate analysis was performed for polar metabolomics and lipidomics separately, however, combining the data from both ionization modes. PCA-X modelling revealed narrow clustering of QC-samples and one outlier for the polar metabolomics strategy (Fig. 3). Moreover, natural patterning according to disease classification was observed and confirmed by OPLS-DA modelling: a $Q^2(Y)$ of 0.800, valid permutation testing, and a *p*-value of $1.43e^{-10}$ for polar metabolomics; a $Q^2(Y)$ of 0.665, valid permutation testing, and a *p*-value of $4.11e^{-5}$ for lipidomics. Using a 20%-leave-out validation strategy, a general classification accuracy of 95.1% and 90.5% was obtained for polar metabolomics and lipidomics fingerprinting, respectively. Considering both strategies, accuracy values were ≥85.7% for the sensitivity and ≥95.2% for the specificity. Following this, components with marker potential were selected based on the VIP-score (> 1), Jackknifed confidence interval (not across zero), and S-plot data (correlation |pcorr| > 0.5, covariance |p| > 0.03 or > 0.015) (Fig. 3). This rendered 45 and 54 potential markers for the polar metabolomics and lipidomics fingerprinting strategy, respectively (Supplemental Table 2).

3.3. Identification of potential UHPLC-HRMS metabolite markers

For the defined markers, identification was pursued, thereby using retention time and accurate mass (MS^1) and precursor-specific fragmentation data (MS^2) as orthogonal data sources [20]. One particular finding related to the fact that the majority of the most prominent markers (top 20) could be linked to metformin (Supplemental Fig. 1). Linkage was noted to relate to either metformin in-source fragmentation and variant adduct formation (Supplemental Fig. 2) or metformin metabolization by the host or residing microbial community (Table 1, Fig. 4, and Supplemental Fig. 3). However, it was verified that valid OPLS-DA models ($Q^2Y \geq 0.619$ and *p*-value ≤ 0.0012) could also be constructed after removal of the assumed metformin-related data fraction.

4. Discussion

LA-REIMS metabolic fingerprinting. In this study, we established LA-REIMS for rapid metabolic fingerprinting of feces and provided proof-of-concept for its discrimination capabilities in a cohort of healthy individuals and type 2 diabetes patients. Whereas previous applications of this ambient ionization technique were mainly focused on surgical interventions and tissue-based fingerprinting [1,8,9], the fitness of LA-REIMS was now also demonstrated for a biofluid, thereby performing cross-platform evaluation with UHPLC-HRMS in terms of metabolome coverage and metabolic segregation according to disease classification.

With respect to the metabolome coverage, LA-REIMS signals were generated based on mass spectral measurements at the surface (*i.e. m/z*-values), which implicates that isomeric and isobaric compounds are manifested through a conjunct signal. The lack of orthogonal data may thus confine the metabolome coverage, as well as complicate data interpretation since deconvolution is hampered. Nevertheless, in this study, the established LA-REIMS fecal fingerprints allowed significant discrimination according to disease classification, which was substantiated by a validated OPLS-DA model and general classification accuracy. In this context, it should be noted that significant discrimination (OPLS-DA; Q^2 of 0.625 and p-value of $4.11\ e^{-6}$) was also achieved when only the LA-REIMS data from the second sampling campaign was used. As such, similar discriminative performance as for UHPLC-HRMS fingerprinting was concluded. It may be raised that the metabolome as covered by LA-REIMS analysis still contained a significant fraction of biologically relevant metabolites, able to achieve clustering of samples according to disease classification. In this regard, it should be mentioned that steps of sample pre-treatment, extraction, and chromatographic separation are generally excluded in case of LA-REIMS, for which it may be presumed that the inherent metabolome composition captured is more representative for the biofluid. In this study, only lyophilized samples were available, which implies that

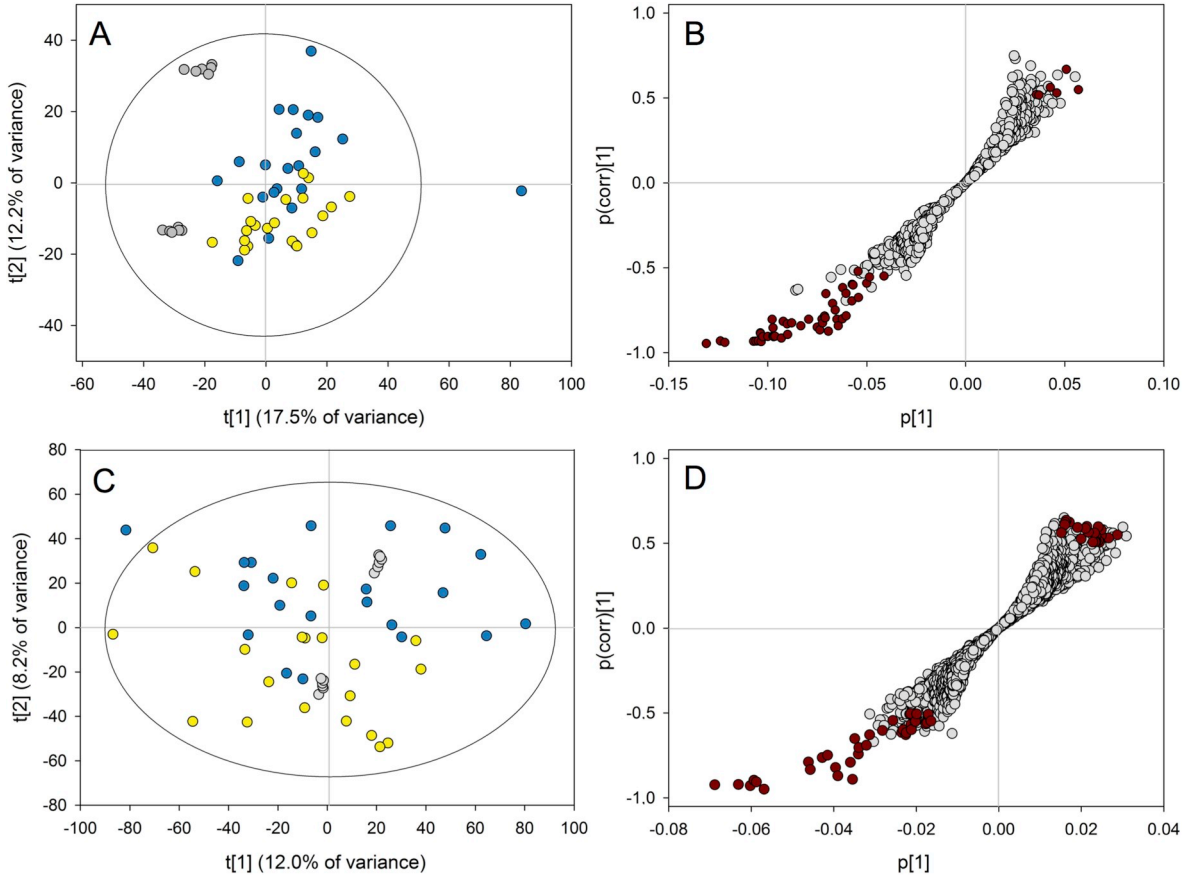

Fig. 3. Discriminative performance of UHPLC-HRMS fecal fingerprinting in type 2 diabetes. PCA-X score plots that were generated based on the polar metabolomics (A) and lipidomics (C) UHPLC-HRMS data, as obtained from the type 2 diabetes study participants (blue) and controls (yellow). Following OPLS-DA modelling, metabolite compounds with marker potential were selected based on the VIP-scores, Jack-knifed confidence intervals, and S-plot data (C and D, polar metabolomics and lipidomics, respectively). (For interpretation of the references to colour in this figure legend, the reader is referred to the Web version of this article.)

spatial metabolic differences of the stool samples [27] were not able to exert any influence. In this regard, when fresh stool material would be used, it may be advisable to use bio sampling blender bags (*e.g.* Stomacher®) and optimized repeated measurement patterns to minimize the impact of biological intra-sample variation. Moreover, in this study, the lyophilization procedure and subsequent reconstitution of the fecal dry matter in ultrapure water rendered a constant water percentage (75%) across samples. However, in real point-of-care applications, this will not be the case as LA-REIMS will be applied to fresh samples. Therefore, to take into account sample dilution, the implementation of appropriate strategies such as probabilistic quotient normalization may be designated [28]. Although TIC-normalization may also be a valid choice, this approach may have some significant shortcomings when large differences in the metabolic fingerprints between the studied disease classifications would be present.

Identification of potential UHPLC-HRMS metabolite markers. An in-depth UHPLC-HRMS strategy for clinical qualification similarly to the one effectuated in this study is proposed. Following UHPLC-HRMS data interpretation, it was rather evident that metformin appeared as a key marker molecule since this drug was prescribed to all participating type 2 diabetes patients (other medications were not generally prescribed to all patients). Moreover, it was observed that a large part of the

Table 1
Overview of UHPLC-HRMS features that were assigned discriminating potential towards disease classification and (putatively) identified as metformin metabolization products.

m/z (Da)	Ion	R_t (min)	Chemical formula	Relevant fragments	Identification
130.108	$[M+H]^+$	1.08	$C_4H_{11}N_5$	55.02, 56.03, 60.06, 68.02, 71.06, 85.05, 88.08, 96.06, 113.08	Metformin (Tier 1)
160.122	$[M+H]^+$	1.55	$C_5H_{13}N_5O$	60.06, 71.06, 85.05, 88.05, 113.08, 130.11, 142.11	CID 72700518 (Tier 3)
184.119	$[M+H]^+$	2.27	$C_7H_{13}N_5O$	68.02, 71.06, 86.07, 113.08, 139.06, 167.09	Triazepinone (Tier 2)
244.139	$[M+H]^+$	1.58	$C_9H_{17}N_5O_3$	60.06, 85.05, 113.08, 130.11, 167.09, 184.12, 199.08, 226.13	Hydroxylated triazepinone (Tier 2)
247.187	$[M+H]^+$	1.22	$C_9H_{22}N_6O_2$	60.05, 112.08, 115.05, 118.09, 126.09, 128.07, 130.11	CID 71333681 (Tier 3)
259.209	$[M+H]^+$	1.03	$C_8H_{22}N_{10}$	60.06, 71.06, 85.05, 88.09, 113.08, 130.11	CID 87288714 (Tier 3)
261.202	$[M+H]^+$	0.99	$C_{10}H_{24}N_6O_2$	60.06, 71.06, 130.11, 132.10	Tier 4
274.150	$[M+H]^+$	1.37	$C_{10}H_{19}N_5O_4$	60.06, 70.07, 72.08, 113.08, 130.11, 186.09, 204.10, 256.14	CID 90392511 (Tier 3)
291.213	$[M+H]^+$	1.05	$C_{11}H_{26}N_6O_3$	60.06, 111.04, 129.05, 130.11, 162.11	CID 21534083 (Tier 3)
295.186	$[M+H]^+$	1.09	$C_{13}H_{22}N_6O_2$	60.06, 71.06, 88.09, 130.11	CID 71333681 (Tier 3)
498.453	$[M+H]^+$	7.60	$C_{31}H_{55}N_5$	71.06, 81.07, 83.09, 85.05, 88.09, 95.08, 107.09, 109.10, 113.08, 121.10, 135.12, 161.13	Cholesterol-metformin (Tier 2)

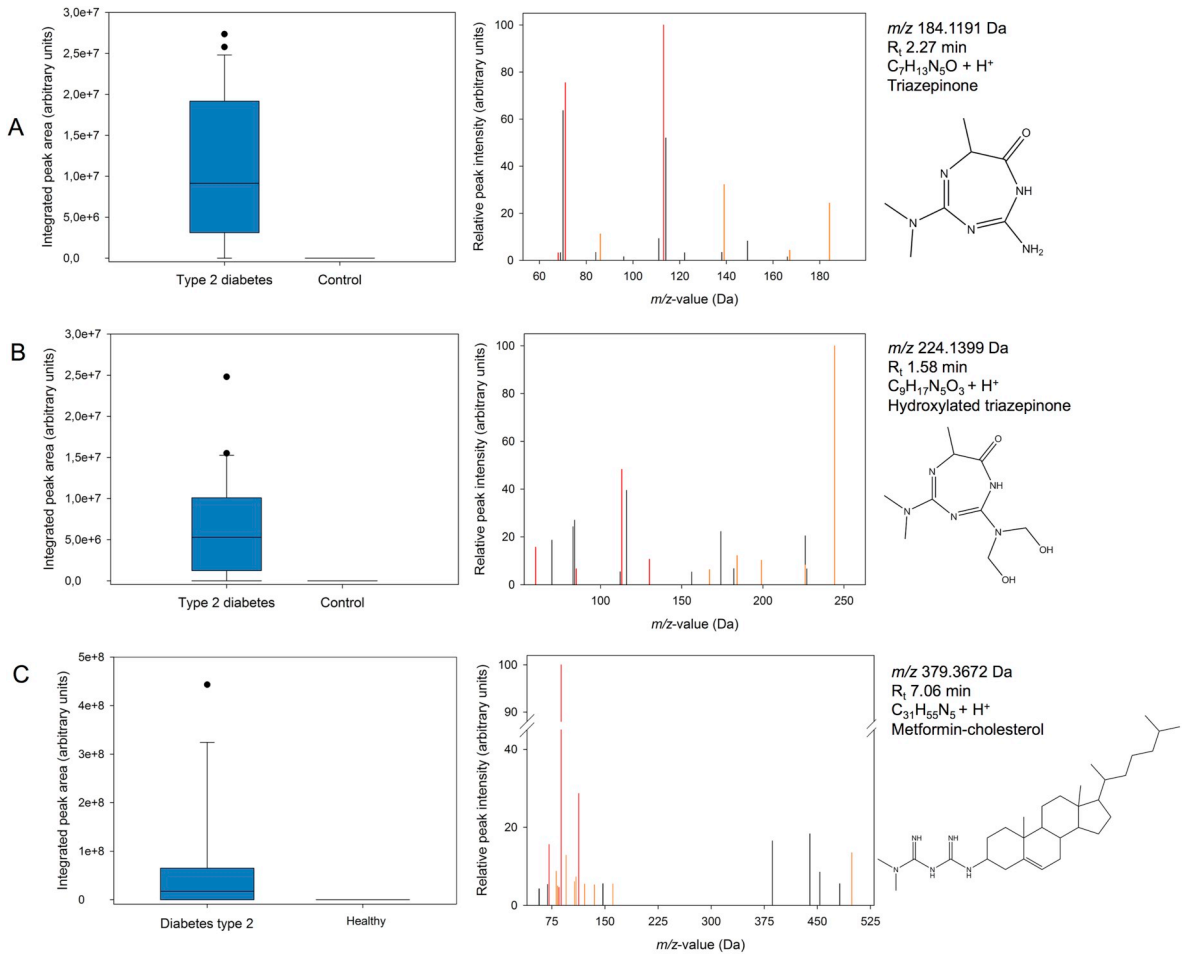

Fig. 4. Metformin metabolization products. Examples of metabolization products of metformin (A, B, C) that were detected in the fecal material of type 2 diabetes patients. Structural analysis was based on the MS^2 spectra, whereby fragments were red when matching the metformin fragmentation tree (Supplemental Fig. 1) and orange when considered relevant for identification. (For interpretation of the references to colour in this figure legend, the reader is referred to the Web version of this article.)

biomarker signature linked to metformin was generated through the process of in-source fragmentation, which implied that these particular compounds comprised no additional clinical marker potential. On the other hand, the remaining compounds that could be linked to metformin were verified as metabolization products of metformin, thus preserving their marker potential.

Triazepinone and its hydroxylation product have been reported earlier by Ruggiero-Lopez et al. (1999) [29], which assessed the reaction of metformin with various α-dicarbonyl compounds (i.e. glyoxal and methylglyoxal) *in vitro*, to define the potential of metformin to inhibit the formation of advanced glycation end products. The formation of these products is considered as one of the main pathogenic mechanisms leading to chronic vascular and neuropathic complications in type 2 diabetes. Besides the endogenous formation and dietary intake of AGEs, these can be produced and metabolized intraluminally by the gut microbiome as well and have been postulated to be sensed by mammalian cells upon secretion, hence triggering inflammatory processes [30].

Accordingly, various studies have reported elevated plasma levels of glyoxal and methylglyoxal in type 2 diabetes patients, showing strong correlations with glycemic control [31,32]. The *in vitro* experiments were able to substantiate the hypothesized dicarbonyl-scavenging potential of metformin, whereby triazepinone and non-methylated triazepinone were identified as main reaction products, being the result of the condensation between metformin and, respectively, methylglyoxal or glyoxal. In the follow-up *in vivo* study [33], triazepinone was also detected in plasma and urine of type 2 diabetes patients that were treated with metformin. Similarly, our study detected triazepinone in feces of metformin-treated diabetes patients. Besides, our study indicated the presence of a compound that was structurally very similar to triazepinone, for which a hydroxyl substitution of two methyl moieties was supposed. This hydroxylation product has not been reported for blood or urine, suggesting the specific involvement of gut microbial hydroxylases [34]. Therefore, a regulating role of the microbiome in metformin-driven carbonyl detoxification is proposed.

Another highly interesting fecal marker that was uncovered in our study was identified as the condensation product of metformin and cholesterol, whereby the fragmentation pattern of this product (Fig. 4) showed a high degree of correspondence with the fragments that were obtained upon separate injection of the metformin and cholesterol reference standard (Supplemental Figs. 1 and 4). To the best of our knowledge, this compound has not been reported earlier in any *in vitro* or *in vivo* study, dedicated to metformin metabolization. In this context, meta-analysis of randomized-controlled clinical trials suggested that intensive metformin treatment is able to reduce total and LDL-cholesterol in plasma [35], whereby the main hypothesis states that metformin mediates the synthesis of polyunsaturated fatty acids (*i.e.* arachidonic acid) through the AMPK pathway in the liver, affecting membrane fluidity and LDL-cholesterol receptor recycling [36]. Our findings suggest a secondary mode of action that is based on the sequestration of cholesterol by metformin and its subsequent fecal excretion. Hereby, it should be noted that we could not detect this

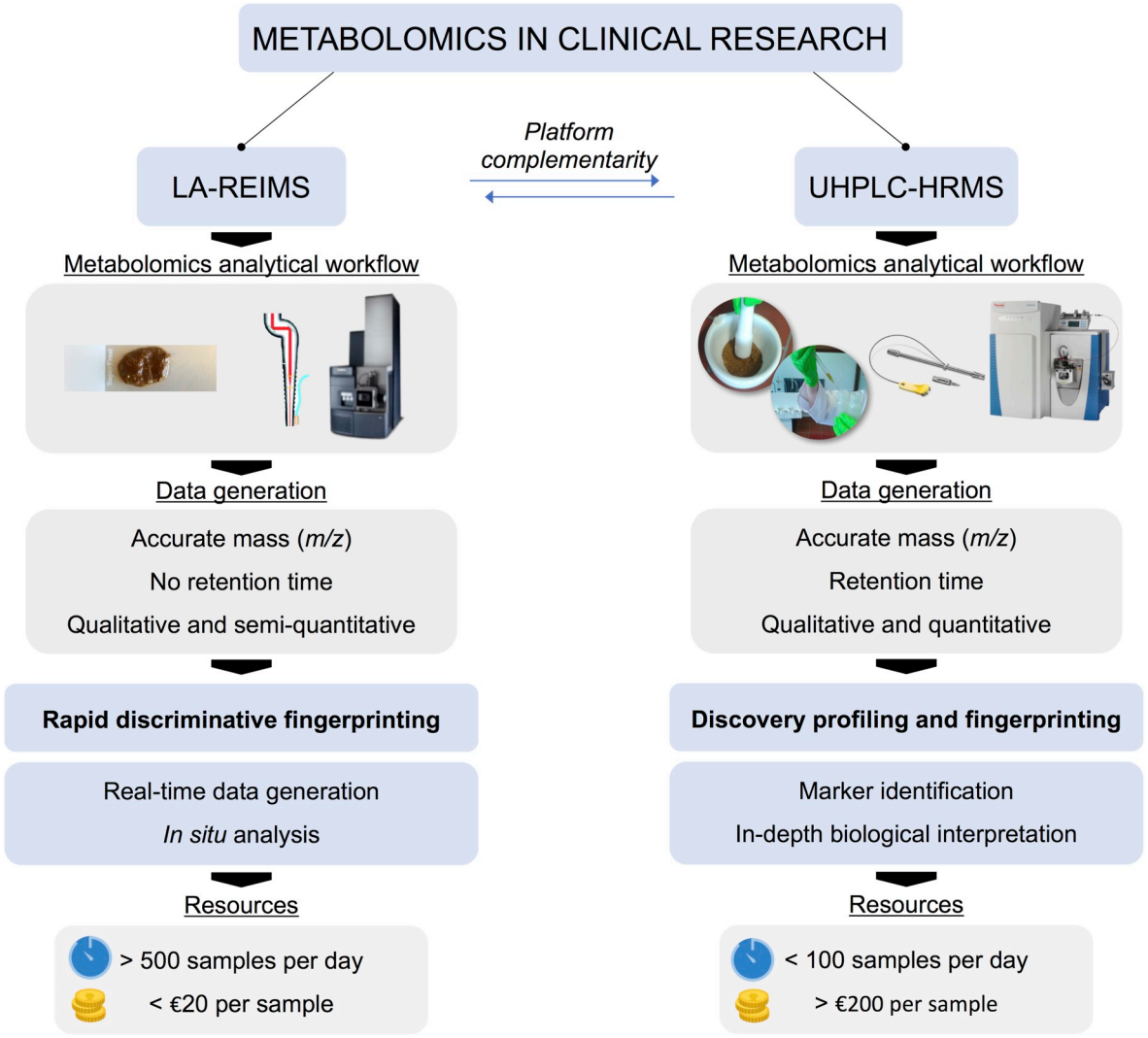

Fig. 5. LA-REIMS and UHPLC-HRMS for metabolomics in precision medicine. Conceptualization of the complementarity between LA-REIMS for rapid discriminative fingerprinting and UHPLC-HRMS for in-depth metabolite characterization and biological interpretation. Estimated costs per sample included consumable, instrument depreciation, and personnel. (Icons were from www.flaticon.com).

condensation product in plasma, as was verified by the analysis of 19 plasma samples from metformin-treated patients. As such, mediation by the gastrointestinal microbial community or hepatic recirculation and biotransformation are proposed as probable molecular mechanisms explaining this condensation reaction. These results are in concordance with Forslund et al. [37] who demonstrated partial gut microbial mediation of both therapeutic and adverse effects of the most widely used antidiabetic medication, metformin.

In conclusion, this study was able to specifically demonstrate the suitability of LA-REIMS for rapid fingerprinting of feces and adequate metabotyping in a context of type 2 diabetes mellitus. These findings further substantiate the potential of LA-REIMS for, in general, rapid biofluid fingerprinting (*e.g.* using saliva, urine, plasma, and serum) with possibilities to differentiate in health and disease. Nevertheless, UHPLC-HRMS remains essential when pursuing in-depth metabolite characterization and biological interpretations. In this study, novel mechanisms of metformin action were elucidated, based on the identification of known and previously unknown metabolic derivates. As such, the complementary use of LA-REIMS and UHPLC-HRMS is considered an important concept to establish metabolomics in a clinical environment, as conceptualized in Fig. 5.

CRediT authorship contribution statement

Lieven Van Meulebroek: Conceptualization, Methodology, Formal analysis, Investigation, Resources, Writing - original draft, Visualization, Funding acquisition. **Simon Cameron:** Conceptualization, Methodology, Writing - review & editing. **Vera Plekhova:** Methodology, Investigation. **Margot De Spiegeleer:** Methodology, Investigation, Visualization. **Kathleen Wijnant:** Methodology. **Nathalie Michels:** Writing - review & editing, Funding acquisition. **Stefaan De Henauw:** Writing - review & editing, Funding acquisition. **Bruno Lapauw:** Writing - review & editing, Funding acquisition, Conceptualization. **Zoltan Takats:** Conceptualization, Writing - review & editing. **Lynn Vanhaecke:** Conceptualization, Writing - review & editing, Funding acquisition, Supervision.

Declaration of competing interest

The authors declare that they have no known competing financial interests or personal relationships that could have appeared to influence the work reported in this paper.

Acknowledgements

We would like to thank Vicky De Clippele, Charlotte Salens, Dirk Stockx and Beata Pomian for their contribution with respect to the UHPLC-HRMS analyses and data interpretation.

Appendix A. Supplementary data

Supplementary data to this article can be found online at https://doi.org/10.1016/j.talanta.2020.121043.

Funding

This work was supported by VLAIO (grant number IM 150740 – A16/OC/0006), UGent BOF GOA (grant number 2017/000102), FWO Hercules (grant number AUGE/17/09), and FWO ERC Runner-up (grant number G0G0119N). The funding source had no involvement in the study design, writing of the report, or decision to submit the article for publication.

References

[1] L.H. Li, H.Y. Hsieh, C.C. Hsu, Clinical application of ambient ionization. mass spectrometry, Mass Spectrom. 6 (2017) S0060, https://doi.org/10.5702/massspectrometry.S0060.
[2] P.L. Kole, G. Venkatesh, J. Kotecha, R. Sheshala, Recent advances in sample preparation techniques for effective bioanalytical methods, Biomed. Chromatogr. 25 (2011) 199–217, https://doi.org/10.1002/bmc.1560.
[3] D. Vuckovic, Current trends and challenges in sample preparation for global metabolomics using liquid chromatography-mass spectrometry, Anal. Bioanal. Chem. 403 (2012) 1523–1548, https://doi.org/10.1007/s00216-012-6039-y.
[4] C.R. Ferreira, K.E. Yannell, A.K. Jarmusch, V. Pirro, Z. Ouyang, R.G. Cooks, Ambient ionization mass spectrometry for point-of-care diagnostics and other clinical measurements, Clin. Chem. 62 (2016) 99–110, https://doi.org/10.1373/clinchem.2014.237164.
[5] National Institutes of Health, Point-of-care diagnostic testing, Fact Sheet – 2010, (2010).
[6] L.S. Eberlin, I. Norton, A.L. Dill, A.J. Golby, K.L. Ligon, S. Santagata, R.G. Cooks, N.Y.R. Agar, Classifying human brain tumors by lipid imaging with mass spectrometry, Canc. Res. 72 (2012) 645–655, https://doi.org/10.1158/0008-5472.CAN-11-2465.
[7] D. Calligaris, D. Caragacianu, X. Liu, I. Norton, C.J. Thompson, Application of desorption electrospray ionization mass spectrometry imaging in breast cancer margin analysis, Proc. Natl. Acad. Sci. U.S.A. 111 (2014) 15184–15189, https://doi.org/10.1073/pnas.1408129111.
[8] J. Balog, S. Kumar, J. Alexander, O. Golf, J. Huang, T. Wiggins, N. Abbassi-ghadi, A. Enyedi, S. Kacska, J. Kinross, G.B. Hanna, J.K. Nicholson, Z. Takats, *In vivo* endoscopic tissue identification by rapid evaporative ionization mass spectrometry (REIMS), Angew 4032 (2015) 11059–11062, https://doi.org/10.1002/anie.201502770.
[9] C.M. Alfaro, A.K. Jarmusch, V. Pirro, K.S. Kerian, T.A. Masterson, L. Cheng, R.G. Cooks, Ambient ionization mass spectrometric analysis of human surgical specimens to distinguish renal cell carcinoma from healthy renal tissue, Anal. Bioanal. Chem. 408 (2016) 5407–5414, https://doi.org/10.1007/s00216-016-9627-4.
[10] K.-C. Schäfer, J. Dénes, K. Albrecht, T. Szaniszló, J. Balog, R. Skoumal, M. Katona, M. Tóth, L. Balogh, Z. Takats, *In vivo*, in situ tissue analysis using rapid evaporative ionization mass spectrometry, Angew. Chem. Int. Ed. 48 (2009) 8240–8242, https://doi.org/10.1002/anie.200902546.
[11] B. Fatou, P. Saudemont, E. Leblanc, D. Vinatier, V. Mesdag, M. Wisztorski, C. Focsa, M. Salzet, M. Ziskind, M, I. Fournier, *In vivo* real-time mass spectrometry for guided surgery application, Sci. Rep. 6 (2016) 25919, https://doi.org/10.1038/srep25919.
[12] L. Nayak, I. Ray, R.K. De, Precision medicine with electronic medical records: from the patients and for the patients, Ann. Transl. Med. 4 (2016) S61, https://doi.org/10.21037/atm.2016.10.40.
[13] T. Kuo, E.P. Dutkiewicz, J. Pei, C. Hsu, Ambient ionization mass spectrometry today and tomorrow: embracing challenges and opportunities, Anal. Chem. 92 (2020) 2353–2363, https://doi.org/10.1021/acs.analchem.9b05454.
[14] F.J. Martin, N. Sprenger, I. Montoliu, S. Rezzi, S. Kochhar, J.K. Nicholson, Dietary modulation of gut functional ecology studied by fecal metabonomic, J. Proteome Res. 9 (2010) 5284–5295, https://doi.org/10.1021/pr100554m.
[15] S. Matysik, C.I. Le Roy, G. Liebisch, S.P. Claus, Metabolomics of fecal samples: a practical consideration, Trends Food Sci. Technol. 57 (2016) 244–255, https://doi.org/10.1016/j.tifs.2016.05.011.
[16] J. Vanden Bussche, M. Marzorati, D. Laukens, L. Vanhaecke, Validated high resolution mass spectrometry-based approach for metabolomic fingerprinting of the human gut phenotype, Anal. Chem. 87 (2015) 10927–10934, https://doi.org/10.1021/acs.analchem.5b02688.
[17] L. Van Meulebroek, E. De Paepe, V. Vercruysse, B. Pomian, S. Bos, B. Lapauw, L. Vanhaecke, Holistic lipidomics of the human gut phenotype using validated ultra-high-performance liquid chromatography coupled to hybrid Orbitrap mass spectrometry, Anal. Chem. 89 (2017) 12502–12510, https://doi.org/10.1021/acs.analchem.7b03606.
[18] N. Verougstraete, B. Lapauw, S. Van Aken, J. Delanghe, C. Stove, V. Stove, Volumetric absorptive microsampling at home as an alternative tool for the monitoring of HbA1c in diabetes patients, Clin. Chem. Lab. Med. 55 (2017) 462–469, https://doi.org/10.1515/cclm-2016-0411.
[19] R. Di Guida, J. Engel, J.W. Allwood, R.J.M. Weber, M.R. Jones, U. Sommer, M.R. Viant, W. B Dunn, Non-targeted UHPLC-MS metabolomic data processing methods: a comparative investigation of normalisation, missing value imputation, transformation and scaling, Metabolomics 12 (2016) 1–14, https://doi.org/10.1007/s11306-016-1030-9.
[20] J. Godzien, M. Ciborowski, S. Angulo, C. Barbas, From numbers to a biological sense: how the strategy chosen for metabolomics data treatment may affect final results. A practical example based on urine fingerprints obtained by LC-MS, Electrophoresis 34 (2013) 2812–2826, https://doi.org/10.1002/elps.201300053.
[21] L. Eriksson, J. Trygg, S. Wold, CV-ANOVA for significance testing of PLS and OPLS® models, J. Chemometr. 22 (2008) 594–600, https://doi.org/10.1002/cem.1187.
[22] E. De Paepe, L. Van Meulebroek, C. Rombouts, S. Huysman, K. Verplanken, B. Lapauw, J. Wauters, L.Y. Hemeryck, L. Vanhaecke, A validated multi-matrix platform for metabolomic fingerprinting of human urine, feces and plasma using ultra-high performance liquid-chromatography coupled to hybrid orbitrap high-resolution mass spectrometry, Anal. Chim. Acta 1033 (2018) 108–118, https://doi.org/10.1016/j.aca.2018.06.065.
[23] M.A. Kamleh, T.M.D. Ebbels, K. Spagou, P. Masson, E.J. Want, Optimizing the use of quality control samples for signal drift correction in large-scale urine metabolic profiling studies, Anal. Chem. 84 (2012) 2670–2677, https://doi.org/10.1021/ac202733q.
[24] L.W. Sumner, A. Amberg, D. Barrett, M.H. Beale, R. Beger, C.A. Daykin, T.W.-M. Fan, O. Fiehn, R. Goodacre, J.L. Griffin, T. Hankemeier, N. Hardy, R. Higashi, J. Kopka, A.N. Lane, J.C. Lindon, P. Marriott, A.W. Nicholls, M.D. Reily, J.J. Thaden, M.R. Viant, Proposed minimum reporting standards for chemical analysis, Metabolomics 3 (2007) 211–221, https://doi.org/10.1007/s11306-007-0082-2.
[25] S. Wiklund, E. Johansson, L. Sjöström, E.J. Mellerowicz, U. Edlund, J.P. Shockcor, J. Gottfries, T. Moritz, J. Trygg, Visualization of GC/TOF-MS-based metabolomics data for identification of biochemically interesting compounds using OPLS class models, Anal. Chem. 80 (2008) 115–122, https://doi.org/10.1021/ac0713510.
[26] M. Olah, C. Bologa, T.I. Oprea, An automated PLS search for biologically relevant QSAR descriptors, J. Comput. Aided Mol. Des. 18 (2015) 437–449, https://doi.org/10.1007/s10822-004-4060-8.
[27] J. Gratton, J. Phetcharaburanin, B.H. Mullish, H.R.T. Williams, M. Thursz, J.K. Nicholson, E. Holmes, J.R. Marchesi, J.V. Li, Optimized sample handling strategy for metabolic profiling of human feces, Anal. Chem. 88 (2016) 4661–4668, https://doi.org/10.1021/acs.analchem.5b04159.
[28] F. Dieterle, A. Ross, G. Schlotterbeck, H. Senn, Probabilistic quotient normalization as robust method to account for dilution of complex biological mixtures. Application in 1H NMR metabonomics, Anal. Chem. 78 (2016) 4281–4290, https://doi.org/10.1021/ac051632c.
[29] D. Ruggiero-Lopez, S. Howell, B. Szwergold, N. Wiernsperger, P. Beisswenger, Metformin reduces methylglyoxal levels by formation of a stable condensation product (triazepinone), Diabetes 49 (2000) A124, https://doi.org/10.4314/tjpr.v18i7.26.
[30] I. Cohen-Or, C. Katz, E.Z. Ron, AGEs secreted by bacteria are involved in the inflammatory response, PloS One 6 (2011) e17974, , https://doi.org/10.1371/journal.pone.0017974.
[31] K.J. Knecht, M.S. Feather, J.W. Baynes, Detection of 3-deoxyfructose and 3-deoxyglucosone in human urine and plasma: evidence for intermediate stages of the Maillard reaction *in vivo*, Arch. Biochem. Biophys. 294 (1992) 130–137, https://doi.org/10.1016/0003-9861(92)90146-N.
[32] A.C. McLellan, S.A. Philips, P.J. Thornalley, The assay of methylglyoxal in biological systems by derivatization with 1,2-diamino-4,5-dimethoxybenzene, Anal. Biochem. 206 (1992) 17–23, https://doi.org/10.1016/S0003-2697(05)80005-3.
[33] P.J. Beisswenger, S.K. Howell, A.D. Touchette, S. Lal, B.S. Szwergold, Metformin reduces systemic methylglyoxal levels in type 2 diabetes, Diabetes 48 (1999) 198–202, https://doi.org/10.2337/diabetes.48.1.198.
[34] A. Whang, R. Nagpal, H. Yadav, Bi-directional drug-microbiome interactions of anti-diabetics, EBioMedicine 39 (2019) 591–602, https://doi.org/10.1016/j.ebiom.2018.11.046.
[35] M.G. Wulffelé, A. Kooy, D. De Zeeuw, C.D.A. Stehouwer, R.T. Gansevoort, The effect of metformin on blood pressure, plasma cholesterol and triglycerides in type 2 diabetes mellitus: a systematic review, J. Intern. Med. 256 (2004) 1–14, https://doi.org/10.1111/j.1365-2796.2004.01328.x.
[36] T. Xu, S. Brandmaier, A.C. Messias, C. Herder, H.H.M. Draisma, A. Demirkan, Z. Yu, J.S. Ried, T. Haller, M. Heier, M. Campillos, G. Fobo, R. Stark, C. Holzapfel, J. Adam, S. Chi, M. Rotter, T. Panni, A.S. Quante, Y. He, C. Prehn, W. Roemisch-Margl, G. Kastenmüller, G. Willemsen, R. Pool, K. Kasa, K. Willems van Dijk, T. Hankemeier, C. Meisinger, B. Thorand, A. Ruepp, M. Hrabé de Angelis, Y. Li, H.-E. Wichmann, B. Stratmann, K. Strauch, A. Metspalu, C. Gieger, K. Suhre, J. Adamski, T. Illig, W. Rathmann, M. Roden, A. Peters, C.M. van Duijn, D.I. Boomsma, T. Meitinger, R. Wang-Sattler, Effects of metformin on metabolite profiles and LDL cholesterol in patients with type 2 diabetes, Diabetes Care 38 (2015) 1858–1867, https://doi.org/10.2337/dc15-0658.
[37] K. Forslund, F. Hildebrand, T. Nielsen, G. Falony, E. Le Chatelier, S. Sunagawa, E. Prifti, S. Vieira-Silva, V. Gudmundsdottir, H.K. Pedersen, M. Arumugam, K. Kristiansen, A.Y. Voigt, H. Vestergaard, R. Hercog, P.I. Costea, J.R. Kultima, J. Li, T. Jorgensen, F. Levenez, J. Dore, MetaHIT consortium, H.B. Nielsen, S. Brunak, J. Raes, T. Hansen, J. Wang, S.D. Ehrlich, P. Bork, O. Pedersen, Disentangling type 2 diabetes and metformin treatment signatures in the human gut microbiota, Nature 528 (2015) 262–266, https://doi.org/10.1038/nature15766.